Elevation Dependency of the Surface Climate Change Signal: A Model Study

FILIPPO GIORGI, JAMES W. HURRELL, AND MARIA ROSARIA MARINUCCI

*National Center for Atmospheric Research, Boulder, Colorado**

MARTIN BENISTON

Swiss Federal Institute of Technology, Zurich, Switzerland

(Manuscript received 22 March 1996, in final form 19 June 1996)

ABSTRACT

Results are presented from a present-day and a doubled CO_2 experiment over the Alpine region with a nested regional climate model. The simulated temperature change signal shows a substantial elevation dependency, mostly during the winter and spring seasons, resulting in more pronounced warming at high elevations than low elevations. This is caused by a depletion of snowpack in doubled CO_2 conditions and further enhanced by the snow–albedo feedback. This result is consistent with some observed temperature trends for anomalously warm years over the Alpine region and suggests that high elevation temperature changes could be used as an early detection tool for global warming. Changes in precipitation, as well as other components of the surface energy and water budgets, also show an elevation signal, which may have important implications for impact assessments in high elevation regions.

1. Introduction

Beniston and Rebetez (1996) have proposed that surface climate change associated with global warming might show an elevation signal, whereby the warming at high elevation sites would be more pronounced than at low elevations. Their hypothesis was based on an analysis of wintertime minimum temperature anomalies from 88 Swiss stations, which revealed a significant altitudinal dependency except at low elevation stations, where fog or stratus conditions frequently occurred. The elevation signal in temperature anomaly was especially clear for 39 stations located in the Swiss Alps, which cover more than 60% of the surface area of Switzerland.

Since the late 1980s much of Europe has been under the influence of a strong positive phase of the North Atlantic oscillation (NAO), so that recent winters in Switzerland have been characterized by anomalously high surface pressure, warm temperatures, and significant reductions in precipitation (Beniston et al. 1994; Hurrell 1995; Hurrell and van Loon 1996). Since the climate of Switzerland is strongly influenced by the NAO, changes in temperature associated with changes in the phase of the NAO can be examined as a function of elevation. Figure 1 shows the differences in December–February mean temperatures at 36 Alpine stations (listed in Table 1 of Beniston and Rebetez 1996) based on composites constructed during winters in which the NAO index exceeded a departure of one standard deviation from a long-term mean (high minus low index winters). The temperature changes show a clear dependence on altitude, such that the higher the elevation the greater the warm anomaly during a high NAO index winter. The correlation between the temperature differences and elevation in Fig. 1 is 0.68. As discussed by Beniston and Rebetez (1996), much of the scatter around the trend line is related to local site characteristics.

The issue of elevation dependency of the surface climate change signal is important for a number of reasons. First, an enhancement of high elevation changes in surface climate would imply greater impacts on high altitude ecosystems and hydrologic systems. Second, an amplified response at high elevations could be utilized as an early climate change detection tool. Third, the capability of reproducing the elevation dependency of the climate change signal can provide an important aspect of model verification.

There are different reasons why an elevation dependency of surface climate change can be expected. Beniston and Rebetez (1996) attribute their finding to the fact that high elevation stations are more directly in contact with the free troposphere than low elevation

* The National Center for Atmospheric Research is sponsored by the National Science Foundation.

Corresponding author address: Dr. Filippo Giorgi, NCAR, P.O. Box 3000, Boulder, CO 80307-3000.
E-mail: giorgi@sage.cgd.ucar.edu

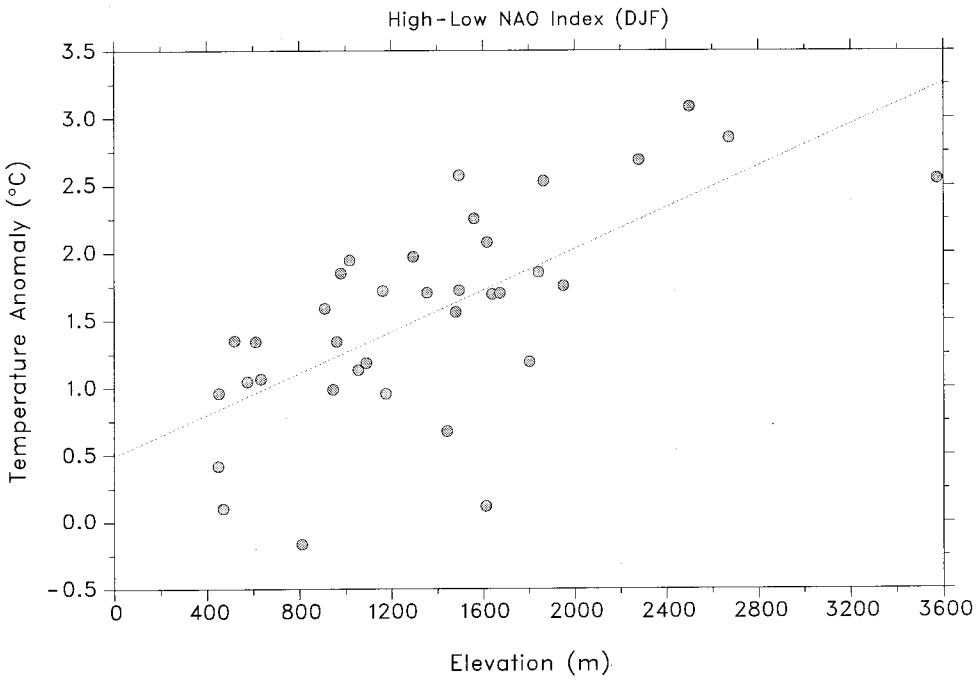

FIG. 1. Difference in winter (December–February) temperature between years with an NAO index ≥ 1.0 standard deviation and those with an index ≤ -1.0 standard deviation as a function of elevation. The NAO index is defined as the difference between the normalized mean winter sea level pressure anomalies at Lisbon, Portugal, and Stykkisholmur, Iceland (see Hurrell 1995), and the index was normalized relative to the 1864–1995 mean. Most of the 36 Alpine stations had complete coverage since the early 1960s, so the composites were formed on temperature records over the period 1960 through 1994. In most cases, this means that 8 high and 8 low NAO index winters were included in the composited means.

ones, and therefore they are less affected by ameliorating anthropogenic factors such as urbanization, pollution, etc. Other physical mechanisms can, however, be important. The snow–albedo feedback provides a strong elevation-dependent forcing. As snow is depleted at high altitudes under warming conditions, the surface albedo decreases, so that more solar radiation is absorbed at the surface and the high elevation surface warming is enhanced. Another physical forcing is associated with precipitation, which may also exhibit an elevation dependency (e.g., Sevruk 1989). Changes in precipitation regimes, therefore, could provide an elevation modulation of the surface climate change signal.

One reason why the topic of elevation dependency of surface climate change has not been the focus of modeling studies is the coarse resolution of most current general circulation models (GCMs). The horizontal resolution of a typical GCM used in climate change studies is of the order of a few hundred kilometers, such that the complex physiography of mountainous areas is excessively smoothed. The development of one-way nested regional climate modeling techniques (e.g., Giorgi and Mearns 1991) allows an increase of horizontal model resolution by over an order of magnitude on the regional scale, so that more realistic regional topographical features can be captured. In this paper we present a study of the elevation dependency of surface climate change using the results from a regional climate simulation over the European region described in Giorgi and Marinucci (1996a, hereafter referred to as GM96). More specifically, we discuss the simulated elevation dependency of surface climate change over the Alpine region and its relationship to changes in the surface energy budget and hydrologic regime. This discussion is presented in section 3 after a brief description of the model and experiment design is given in the following section.

2. Model description and experiment design

GM96 employed a regional climate model (RegCM) developed at the National Center for Atmospheric Research (NCAR) driven by output from a present-day simulation (control run) and a simulation under doubled carbon dioxide concentration ($2 \times CO_2$ run) performed with a version of the NCAR Community Climate Model (CCM) developed by Meehl and Washington (1990) and further modified by Washington and Meehl (1993). This is a variant of the first-generation NCAR CCM run at spectral R15 truncation, which yields a horizontal resolution of approximately 7.5° long $\times$ 4.5° lat. The atmospheric model is coupled to a 50-m mixed-layer ocean model and a one-layer thermodynamic sea–ice formulation. No flux correction terms are included in

the ocean model and the surface hydrology over land is calculated using a bucket-type formulation.

The RegCM is an augmented version of the NCAR/Pennsylvania State University mesoscale model MM4 and is described in detail by Giorgi et al. (1993a,b). It is a primitive equation, gridpoint limited-area model with compressibility and hydrostatic balance. For application to climate studies, a number of physics parameterizations were incorporated in the model, which include a state-of-the-art surface physics package [the Biosphere–Atmosphere Transfer Scheme, or BATS; Dickinson et al. (1993)], an explicit planetary boundary-layer formulation (Holtslag et al. 1990), a detailed atmospheric radiative calculation package (Briegleb 1992), a mass flux cumulus parameterization scheme (Grell et al. 1994), and a simplified explicit moisture scheme including an equation for cloud water (Giorgi and Marinucci 1996b).

Of particular interest for this study is BATS, which is a scheme designed to describe the role of vegetation, snow, and interactive soil moisture in modifying the surface–atmosphere exchanges of momentum, energy, and water vapor. It comprises a vegetation layer, a snow layer, a surface soil layer 10 cm thick, a root zone layer of 1–2-m depth, and a deep soil layer of 5-m depth. Prognostic equations are solved for the temperature of the surface soil layer and of the root zone using a generalization of the force–restore method of Deardorff (1978). In the presence of vegetation, the temperature of canopy air and canopy foliage is calculated diagnostically via an energy balance formulation including sensible, radiative, and latent heat fluxes.

The soil hydrology calculations include predictive equations for the water content of the surface soil layer, the root zone, and the deep soil layer. These equations account for precipitation, snowmelt, canopy foliage drip, evapotranspiration, surface runoff, infiltration below the root zone, and diffusive exchange of water between soil layers. The soil water movement formulation is obtained from a fit to results from a high-resolution soil model and the surface runoff rates are expressed as functions of the precipitation rates and the degree of soil water saturation. The surface evapotranspiration rates depend on the availability of soil water, which is a prognostic variable. Snow depth is prognostically calculated from snowfall, snowmelt, and sublimation. Precipitation is assumed to fall in the form of snow if the temperature at the atmospheric model level closest to the surface is less than 275 K. BATS can currently describe 15 vegetation types. Broad-leaf and needle-leaf forests are the dominant types over the Alpine region.

Figure 2 depicts the RegCM topography for the selected domain, which encompasses most of the European region and portions of the northeastern Atlantic and the Mediterranean. The model was run at 50-km grid point spacing, which yields a resolution sufficient to capture the basic features of the regional European topography and coastlines. By comparison, at R15 resolution the European topography is reduced to a relief of about 400-m height centered over the Alpine region (e.g., see Marinucci and Giorgi 1992). Also shown in Fig. 2 is the Alpine subregion that was selected for detailed analysis in this work. It can be noted that the topography spans a range of 2000 m within this region. In the vertical, the model uses 16 σ levels, with a resolution of $\sigma = 0.1$ in the midtroposphere and a higher resolution in the planetary boundary layer (six levels below about 2000 m).

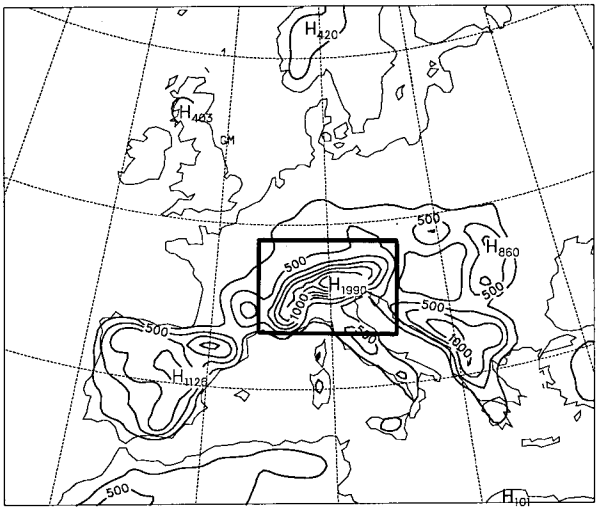

FIG. 2. RegCM domain and topographic field. Units are m, and the contour interval is 250 m. Shown is the Alpine subregion considered in this work.

Two continuous simulations were carried out, a 5-yr present-day run and a 3-yr $2 \times CO_2$ run with the RegCM driven by time-dependent lateral meteorological fields provided from output of CCM simulations. These periods were selected from 50-yr-long CCM equilibrium runs as described by GM96 (for the present-day run). It will be seen that, although the length of these simulations is relatively short (especially for the $2 \times CO_2$ experiment), the magnitude of the warming is so pronounced that the conclusions of this work are qualitatively solid. In addition, as discussed by GM96, the driving CCM run did not show a marked variability between different 5-yr periods. In the RegCM runs, initial soil water content was interpolated from the normalized CCM bucket model water content, and time-dependent SSTs were interpolated from the ocean component of the CCM. All results discussed in the next section are averages over the 5-yr present-day (control) run and the 3-yr $2 \times CO_2$ run calculated only for the Alpine subregion of Fig. 2.

3. Results

a. Biases in the control run over the Alpine region

Washington and Meehl (1993) discuss the CCM simulation used to drive the RegCM runs and GM96 discuss

TABLE 1. Seasonal surface air temperature and precipitation bias over the Alpine subregion (see Fig. 2) in the control run experiment of GM96. Units are °C for temperature and percentage of the observed value for precipitation.

	Winter	Spring	Summer	Fall
Temperature	1.3	−4.1	1.0	−1.3
Precipitation	9.3%	8.6%	−23.7%	0.3%

the overall RegCM performance over the European region for the control run. However, it is useful to briefly summarize the model biases over the Alpine region. Table 1 presents the seasonal surface air temperature and precipitation biases over the Alpine region for the control run. The biases are defined as the difference between simulated and observed regionally and seasonally averaged values. Observations are from Legates and Willmott (1990a,b) and the precipitation biases are expressed as a percentage of the observed values.

The surface air temperature biases are small, order of 1°C, except in spring, when the model is colder than observed by about 4°C, which may be due to excessive spring snow cover (e.g., see Fig. 4). The precipitation biases are also small, less than 10%, except in summer, when the model underpredicts precipitation by about 24%. It should be noted, however, that the Legates and Willmott dataset was produced without including any station elevation correction, so that it is likely biased toward low elevation stations over the Alps. Therefore, the model biases should be viewed within the context of a possible uncertainty in the Legates and Willmott dataset over mountainous areas. The salient point is that the biases of Table 1 indicate that the seasonally averaged temperature and precipitation errors in the present control run experiment are modest.

b. Temperature and the surface energy budget

Figure 3 shows the difference between 2 × CO_2 and control run average surface air temperature as a function of elevation for the four seasons over the model grid points included in the Alpine region. The curves were obtained by grouping grid points based on topographical elevation categories of 100-m intervals, that is, points with topography in the range of 0.1–0.2 km, 0.2–0.3 km, . . . , 1.9–2.0 km, and averaging results over all grid points within each elevation category. The number of grid points in each elevation category is given in Table 2 and varies from a maximum of 38 for elevations between 0.3 and 0.4 km to a minimum of two for the highest elevation categories.

The simulated warming is quite pronounced, with values between 5° and 6.5°C. This is mostly due to the CCM boundary forcing. A recent intercomparison by T. Kittel et al. (1996, manuscript submitted to *Climate Dyn.*) of climate change runs produced with different GCMs has indicated that the latest versions of the Washington–Meehl model show a strong sensitivity to CO_2

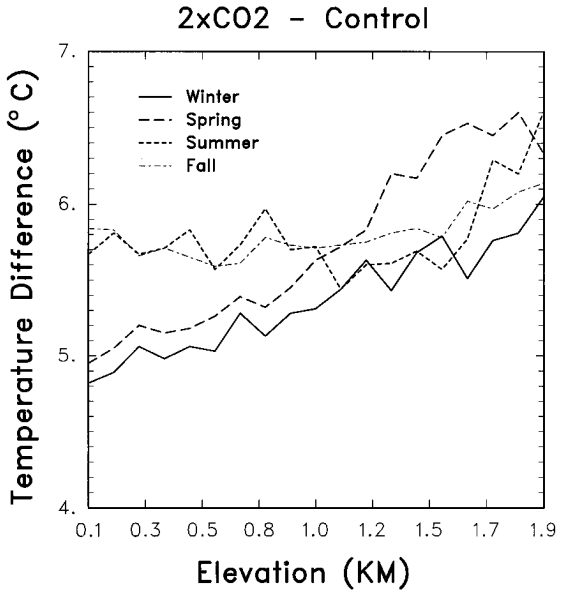

FIG. 3. Difference between 2 × CO_2 and control run surface air temperature as a function of elevation over the Alpine subregion for the four seasons. Units are °C.

concentration. A consequence of this is that the strength of the perturbation decreases the importance of the sample size problems associated with the length of the 2 × CO_2 simulation. As a reference, the gridpoint standard deviations of the seasonal temperatures for the 5-yr control run were in the range of 0.5°–2°C—that is, much smaller than the simulated warming.

A marked elevation signal in simulated warming is found in winter and spring, while the signal is not evident in summer and fall except at very high elevations. This result points directly to the snow–albedo feedback mechanism. Figures 4a,b show the winter and spring

TABLE 2. Number of grid points within the Alpine region used in the averaging for each elevation category used in Figs. 3–10.

Elevation (km)	No. grid points
.1–.2	12
.2–.3	21
.3–.4	38
.4–.5	32
.5–.6	27
.6–.7	19
.7–.8	19
.8–.9	8
.9–1.0	8
1.0–1.1	3
1.1–1.2	7
1.2–1.3	7
1.3–1.4	9
1.4–1.5	5
1.5–1.6	7
1.6–1.7	3
1.7–1.8	3
1.8–1.9	2
1.9–2.0	2

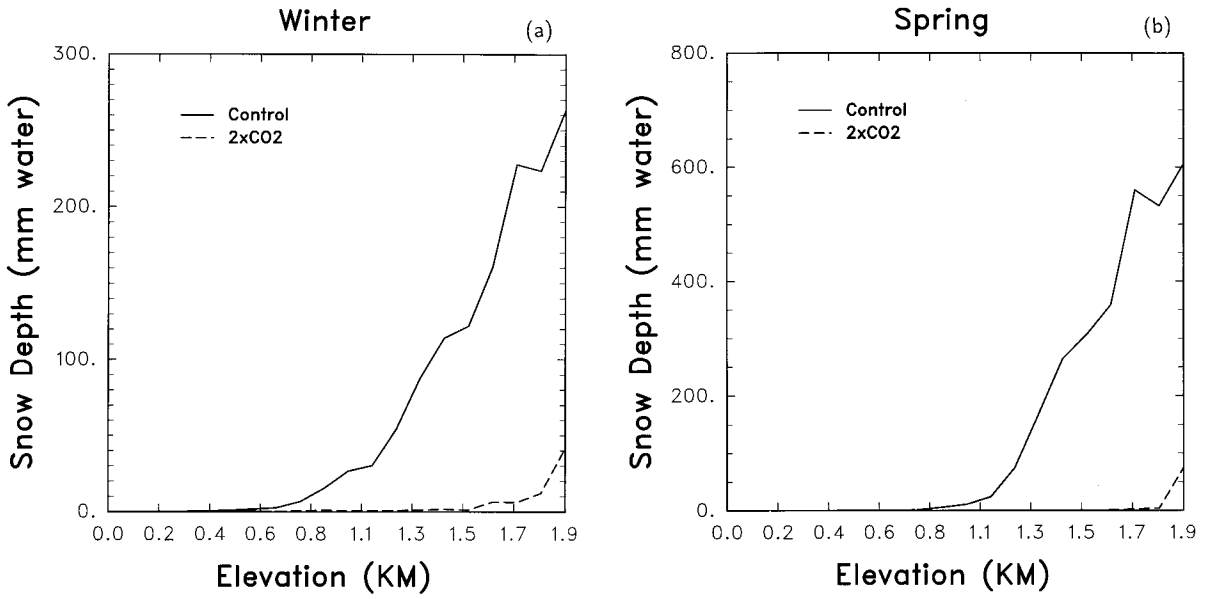

FIG. 4. Snow depth as a function of elevation over the Alpine subregion in the control and 2 × CO_2 experiments: (a) winter; (b) spring. Units are equivalent mm of water.

snow depth as a function of elevation for the control and 2 × CO_2 experiments. In the control run, snow significantly accumulates starting from elevations of 800 m in winter and 1100 m in spring, and the snow depth increases with elevation. Note that the equivalent liquid water snow amounts are greater in spring than in winter. In fall and summer the control run produced very little snow except for some residual summer snow at very high elevations. In the 2 × CO_2 run, snow is entirely depleted except at the highest elevations.

As a result of snow depletion, the 2 × CO_2-control run-solar absorbed flux at the surface shows a strong elevation signal, especially in spring and at high elevations in summer (see Fig. 5). A clear elevation trend is also evident in winter but it has a comparatively low magnitude because of the low winter absolute insolation amounts. The elevation warming trends (Fig. 3) are thus consistent with the trends in solar flux change (Fig. 5) caused by the snow depletion (Fig. 4).

Figures 6 and 7 show the elevation trends of seasonal differences between 2 × CO_2 and control run sensible and latent heat fluxes, respectively. Because of the increased solar radiation flux in 2 × CO_2 conditions at high elevations in spring and summer, both sensible heat and latent heat fluxes increase above about 1000 m in spring and above 1600 m in summer. The elevation increase of these fluxes is substantial, up to 20 W m^{-2} for sensible heat flux and 40–50 w m^{-2} for latent heat flux. Little trend is shown for the other two seasons.

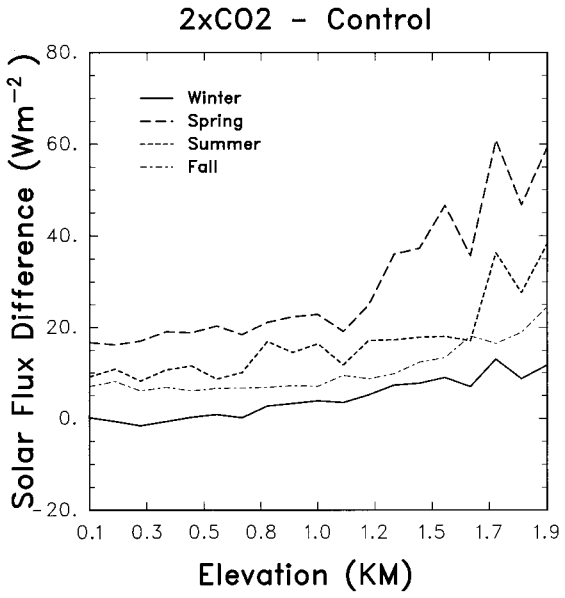

FIG. 5. Difference between 2 × CO_2 and control run absorbed solar flux at the surface as a function of elevation over the Alpine subregion for the four seasons. Units are W m^{-2}.

c. Precipitation and the surface water budget

Precipitation may show an elevation dependency in response to different forcings (e.g., Sevruk 1989; Barry 1994). In the cold season, the dominant contribution is from orographic forcing. This forcing is, however, mostly associated with the gradient of topography rather than topography itself. In fact, during the cold season, precipitation may be expected to decrease at very high elevations because of the scarce availability of water vapor. During summer, topography forces convection

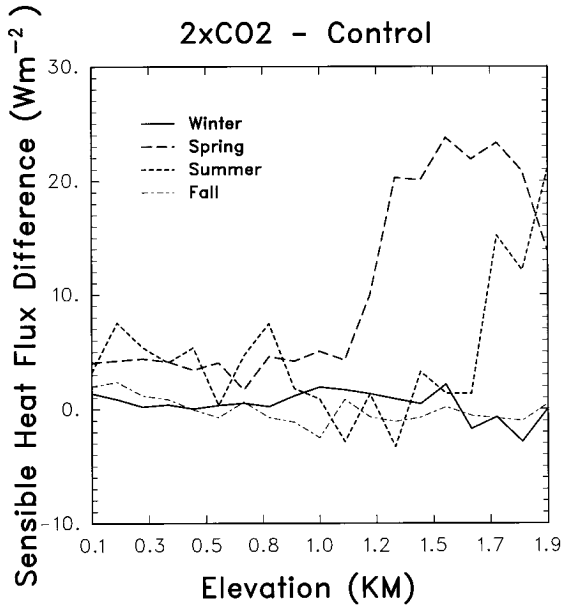

FIG. 6. Difference between 2 × CO_2 and control run surface sensible heat flux as a function of elevation over the Alpine subregion for the four seasons. Units are W m^{-2}.

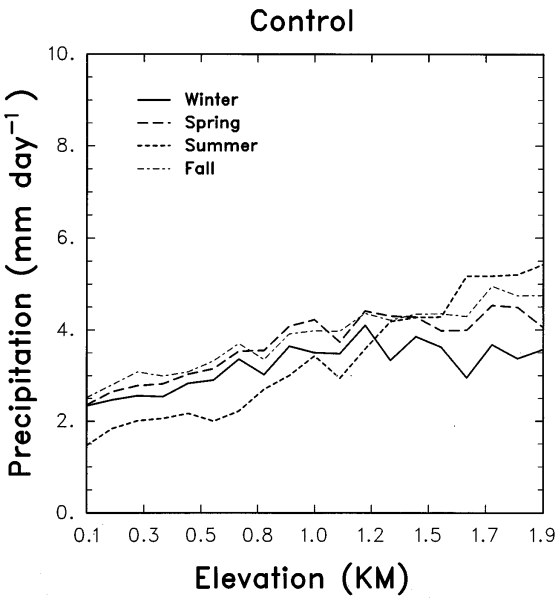

FIG. 8. Control run precipitation as a function of elevation over the Alpine subregion for the four seasons. Units are mm day^{-1}.

through the process of high elevation surface heating, which destabilizes the overlying midtropospheric layers. Topographically induced mesoscale circulations and convergence associated with flow over and around complex topography can also enhance convective precipitation. Some studies have also indicated that summer storm precipitation at the highest elevations of the Rockies may be significantly less than in the foothills (e.g., Myers and Morris 1991).

Figure 8 shows the elevation dependency of seasonal precipitation in the control run. The model shows the most pronounced precipitation sensitivity to elevation during the summer season. This can be expected from the fact that the convective parameterization used in the model (Grell et al. 1994) adopts a closure based on buoyancy production, and thus it is very sensitive to

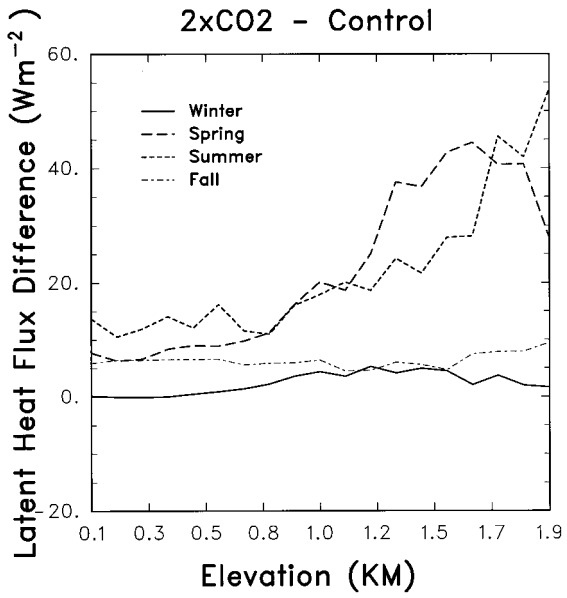

FIG. 7. Difference between 2 × CO_2 and control run surface latent heat flux as a function of elevation over the Alpine subregion for the four seasons. Units are W m^{-2}.

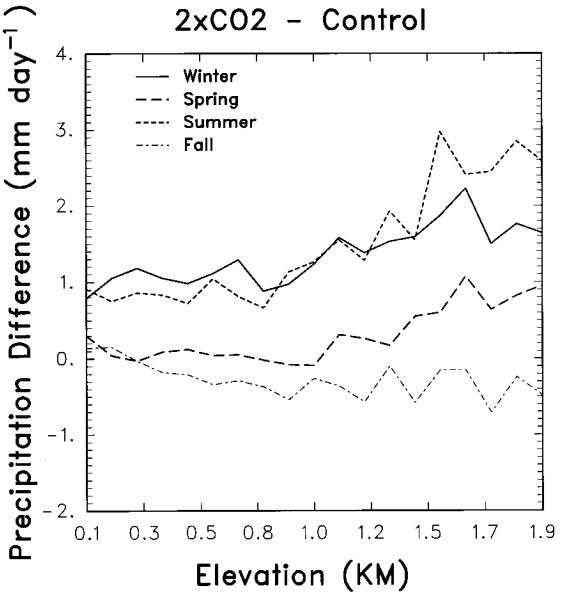

FIG. 9. Difference between 2 × CO_2 and control run precipitation as a function of elevation over the Alpine subregion for the four seasons. Units are mm day^{-1}.

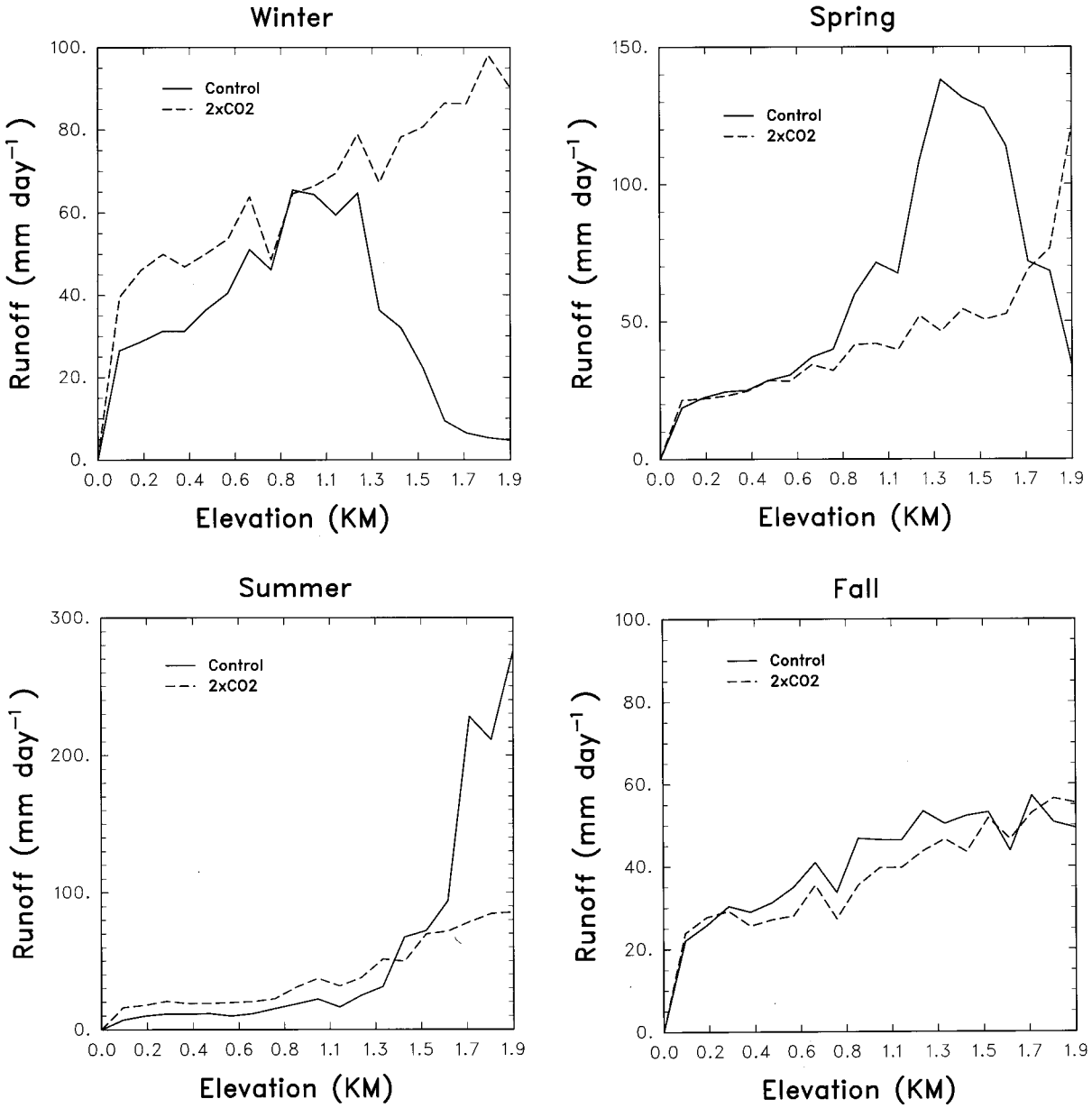

FIG. 10. Surface runoff as a function of elevation over the Alpine subregion in the control and 2 × CO_2 experiments: (a) winter, (b) spring, (c) summer, (d) fall. Units are mm day^{-1}.

surface heating. The simulated elevation dependency of precipitation is less pronounced, although evident, in the other seasons.

Figure 9 presents the difference in 2 × CO_2 and control run precipitation as a function of elevation for the four seasons. Except for the fall, precipitation increased in 2 × CO_2 conditions over the Alpine region. It should be noted that although global warming can generally be expected to lead to a global increase in precipitation, regional precipitation changes are regulated by modifications in large-scale circulation features such as storm track and monsoonal flows. These changes produce shifts in regional precipitation patterns and therefore can lead either to increases or to decreases in regional precipitation amounts.

Summer precipitation shows a marked increase with elevation starting from about 800 m. This is forced by an increase in solar insolation and sensible heat flux (Figs. 5 and 6) and causes the evaporation change trend observed in Fig. 7. The elevation trend in summer precipitation change is also consistent with the pronounced sensitivity of summer convective precipitation to elevation illustrated by Fig. 8. During winter and spring, there is an elevation trend of the simulated 2 × CO_2-

control precipitation change as well, but this is less pronounced than in summer. This result indicates that the main forcing that induces a trend in simulated precipitation change is associated with surface-heating-forced convection. During fall, when overall precipitation decreases over the region, a reversed elevation trend is observed.

Because the $2 \times CO_2$-induced changes in precipitation, evaporation, and snowmelt show significant elevation dependency, it can be expected that changes in other components of the surface hydrologic cycle may be characterized by elevation-dependent trends. Figures 10a–d present control run and $2 \times CO_2$ average surface runoff over the Alpine subregion as a function of elevation for the four seasons. The seasonal migration of the elevation of maximum runoff basically follows the edges of the snowpack. In the control run, the peak runoff zone occurs at 900–1200 m in the winter. As the edge of the snowpack reaches higher elevations in the spring (1300–1500 m), so does the peak runoff zone, while in the summer residual snow melts and runs off only from the highest elevations (1700–2000 m). In the fall, the runoff–elevation trend essentially follows the precipitation trend, since little snow is produced. In the $2 \times CO_2$ simulation, the pattern of runoff–elevation seasonality dependence is entirely modified, mostly as a result of much decreased snowpack formation. In most seasons, runoff follows precipitation and only in the winter and spring some high elevation peak runoff is associated with snowmelt. The changes in runoff patterns also affected soil water content (not shown). In the control run, soil water content maxima were produced in correspondence of the runoff peak regions and seasons, which disappeared in the $2 \times CO_2$ experiments.

4. Summary and discussion

The model results discussed in this work show a significant elevation signal in the simulated temperature and precipitation changes induced by $2 \times CO_2$ warming over the Alpine region, with more pronounced changes at higher elevations. The elevation signal of surface warming is especially marked in the winter and spring seasons, since it is mostly associated with a decrease in snowpack and is thus enhanced by the snow–albedo feedback. Based on these results, we argue that high elevation temperature changes during winter and spring might be used as an early detection tool for global warming.

The simulated elevation trend of surface warming is consistent with the observational analysis of Beniston and Rebetez (1996) and with Fig. 1. Although Beniston and Rebetez did not carry out a detailed analysis of observed snowpack change, they point out how the snowpack during recent winters over the Swiss Alps has been severely depressed as a result of decreased precipitation (Hurrell 1995). This could be an indication of a link between observed temperature and snowpack trends.

Our model also showed a marked elevation signal in the precipitation change, especially during summer. Presently, this result does not have a solid observational counterpart and may be dependent on the convective parameterization used. The convective scheme employed in our model is based on a buoyancy closure and therefore is sensitive to surface heating. Schemes based on different closures, for example, moisture convergence, might have a different response to surface warming. More extensive model experiments and observational analyses are thus required to verify the robustness of this result.

Finally, in addition to temperature and precipitation, other components of the surface energy and water budgets show an elevation signal in the $2 \times CO_2$-induced changes, again mostly driven by the change in snowpack evolution. Most pronounced was the change in the seasonality of peak runoff elevation. This elevation dependency may be important for the assessment of climate change impacts on high altitude ecosystems and water management.

We emphasize that our study should not be viewed as an attempt to quantitatively estimate effects of climate change, but more simply as a sensitivity experiment, which is suggestive of an elevation effect that has an observational counterpart and a proposed physical explanation. More numerical experiments are needed to quantify this effect.

In summary, our results suggest a possible altitudinal dependency of surface climate change, so that continuous and systematic observations at high elevation sites need to be maintained as they may be able to provide tangible measures of global warming. As noted by Beniston and Rebetez (1996), a few century-long records at such sites have already been discontinued for budgetary reasons.

REFERENCES

Barry, R. G., 1994: Past and potential future changes in mountain environments: A review. *Mountain Environments in Changing Climates*, M. Beniston, Ed., Routledge, 3–33.

Beniston, M., and M. Rebetez, 1996: Regional behavior of minimum temperatures in Switzerland for the period 1979–1993. *Theor. Appl. Climatol.,* **53**, 231–244.

——, ——, F. Giorgi, and M. R. Marinucci, 1994: An analysis of regional climate change in Switzerland. *Theor. Appl. Climatol.,* **49,** 135–159.

Briegleb, B. P., 1992: Delta–Eddington approximation for solar radiation in the NCAR Community Climate Model. *J. Geophys. Res.,* **97,** 7603–7612.

Deardoff, J. W., 1978: Efficient prediction of ground surface temperature and moisture with inclusion of a layer of vegetation. *J. Geophys. Res.,* **83,** 1889–1903.

Dickinson, R. E., A. Henderson-Sellers, and P. J. Kennedy, 1993: Biosphere–Atmosphere Transfer Scheme (BATS) Version 1e as Coupled to the NCAR Community Climate Model. NCAR Tech. Note NCAR/TN-387+STR, National Center for Atmospheric Research, Boulder, CO, 72 pp.

Giorgi, F., and L. O. Mearns, 1991: Approaches to the simulation of regional climate change: A review. *Rev. Geophys.,* **29,** 191–216.

——, and M. R. Marinucci, 1996a: Improvements in the simulation

of surface climatology over the European region with a nested modeling system. *Geophys. Res. Lett.,* **23,** 273–276.

——, and ——, 1996b: An investigation of the sensitivity of simulated precipitation to model resolution and its implication for climate studies. *Mon. Wea. Rev.,* **124,** 148–166.

——, ——, and G. T. Bates, 1993a: Development of a second generation regional climate model (RegCM2): Boundary layer and radiative transfer processes. *Mon. Wea. Rev.,* **121,** 2794–2813.

——, ——, G. De Canio, and G. T. Bates, 1993b: Development of a second generation regional climate model (RegCM2): Convective processes and assimilation of lateral boundary conditions. *Mon. Wea. Rev.,* **121,** 2814–2832.

Grell, G. A., J. Dudhia, and D. R. Stauffer, 1994: A description of the fifth generation Penn State/NCAR Mesoscale Model (MM5). NCAR Tech. Note NCAR/TN-398+STR, 121 pp.

Holtslag, A. A. M., E. I. F. de Bruijn, and H. L. Pan, 1990: A high resolution air mass transformation model for short-range weather forecasting. *Mon. Wea. Rev.,* **118,** 1561–1575.

Hurrell, J. W., 1995: Decadal trends in the North Atlantic oscillation regional temperatures and precipitation. *Science,* **269,** 676–679.

——, and H. van Loon, 1996: Decadal variations in climate associated with the North Atlantic oscillation. *Climate Change,* in press.

Legates, D. R., and C. J. Willmott, 1990a: Mean seasonal and spatial variability in gauge-corrected global precipitation. *Int. J. Climatol.,* **10,** 111–127.

——, and ——, 1990b: Mean seasonal and spatial variability in global surface air temperature. *Theor. Appl. Climatol.,* **41,** 11–21.

Marinucci, M. R., and F. Giorgi, 1992: A 2 × CO_2 climate change scenario over Europe generated using a limited area model nested in a general circulation model. Part I: Present day simulation. *J. Geophys. Res.,* **97,** 9989–10 009.

Meehl, G. A., and W. M. Washington, 1990: CO_2 climate sensitivity and snow–sea–ice albedo parameterization in an atmospheric GCM coupled to a mixed-layer ocean model. *Climate Change,* **16,** 283–306.

Myers, V. A., and D. I. Morris, 1991: New techniques and data sources for PMP. *Water Power '91,* D. D. Darling, Ed., American Society of Civil Engineers, 1319–1327.

Sevruk, B., 1989: Reliability of precipitation gradient estimates. *Proc. XIV Int. Conf. on Carpathian Meteorology,* Sofia, Bulgaria, 402–408.

Washington, W. M., and G. A. Meehl, 1993: Greenhouse sensitivity experiments with penetrative cumulus convective and tropical cirrus albedo effects. *Climate Dyn.,* **8,** 211–223.